

# Shadow Navigation Support at JPL for the Rosetta Landing on Comet 67P/Churyumov-Gerasimenko

By Stephen BROSCART,<sup>1)</sup> Shyam BHASKARAN,<sup>1)</sup> Julie BELLEROSE,<sup>1)</sup> Ann DIETRICH,<sup>2)</sup> Dongsuk HAN,<sup>1)</sup> Robert HAW,<sup>1)</sup> Nickolaos MASTRODEMOS,<sup>1)</sup> William OWEN, Jr.,<sup>1)</sup> Brian RUSH,<sup>1)</sup> and David SUROVIK<sup>3)</sup>

<sup>1)</sup>Jet Propulsion Laboratory, California Institute of Technology, California, USA

<sup>2)</sup>University of Colorado - Boulder, Colorado, USA

<sup>3)</sup>Rutgers University, New Jersey, USA

(Received April 17th, 2017)

On September 30, 2016, the European Space Agency's (ESA's) Rosetta spacecraft ended its 12-year mission when it landed on the surface of comet 67P/Churyumov-Gerasimenko (CG). For the preceding 26 months, the spacecraft had characterized the environment of CG in unprecedented detail from a series of orbits and other nearby trajectories. Throughout the mission, the primary navigation responsibility for the mission was handled by ESA's Flight Dynamics team at the European Space Operations Center (ESOC-FD) in Darmstadt, Germany. In order to maximize the probability of a successful landing, ESOC-FD invited a team from the Jet Propulsion Laboratory (JPL) in Pasadena, California to provide independent orbit determination solutions during the last two months of the mission. This paper describes the experiences and results from this JPL "shadow navigation" team.

**Key Words:** comets, navigation, optical navigation, orbit determination

## 1. Introduction

The European Space Agency's (ESA's) Rosetta mission explored the comet 67P/Churyumov-Gerasimenko (CG) in unprecedented detail from its arrival the summer of 2014 through the touchdown and end of mission on Sep. 30, 2016.<sup>1-3)</sup> This mission achieved many mission-operations firsts: the first to rendezvous with a comet, the first to place a lander on the surface of a comet, the first to follow a comet through perihelion, the first to land the main spacecraft bus on a comet, and others. The resulting science yield from the mission has been tremendous.

The Flight Dynamics group at the European Space Operations Center (ESOC-FD) had the responsibility for navigating the Rosetta spacecraft throughout the mission.<sup>4-7)</sup> The Jet Propulsion Laboratory (JPL) Mission Design and Navigation section had the good fortune to be invited to participate in the navigation of Rosetta both during the lead-up to the Philae lander release in Nov. 2014<sup>8,9)</sup> and during the lead-up to the landing of the spacecraft bus that ended the mission. While ESOC-FD retained full responsibility for the spacecraft navigation, the JPL "shadow navigation" team provided an independent orbit determination (OD) solution for the consideration of ESOC-FD.

This paper describes the experiences, results, and lessons learned by the JPL OD team during the 2016 Rosetta mission support. As the ESOC-FD team was so generous with JPL as to invite us to come back and learn more about comet navigation with them, the discussion in this paper shares some of the lessons we learned from the process with the broader navigation community.

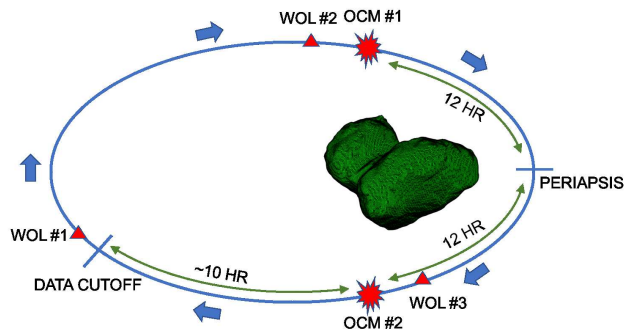


Fig. 1. This operations template was followed for each 3-day orbit between Aug. 10 and Sep. 26, 2016. Not to scale. OCM: Orbit control maneuver, WOL: Reaction wheel offload maneuver.

## 2. Mission Description

For the 2016 support, the JPL team made their first OD delivery on Aug. 1 and continued providing independent solutions about twice a week through the landing on Sep. 30. Detailed context for this period of the mission is available in Accomazzo *et al.*<sup>3)</sup>

At the start of the JPL support, the Rosetta spacecraft was in a terminator orbit with a semi-major axis of roughly 10 km and a periapsis range of about 8.2 km. On Aug. 10, the spacecraft orbit was tilted by 20 deg off of the terminator plane and the orbit period was moved to 3 days. From Aug. 10 through Sep. 26, the 3-day orbit period and orbit plane orientation were maintained and the activities in the orbit followed a regular pattern (Fig. 1).

As time passed in this 3-day orbit, the orbit eccentricity was steadily increased. This had the effect that (almost) each periapsis was lower than the last, which steadily increased the influence of the irregular mass distribution of CG on the spacecraft dynamics. The spacecraft range to the comet as a function time

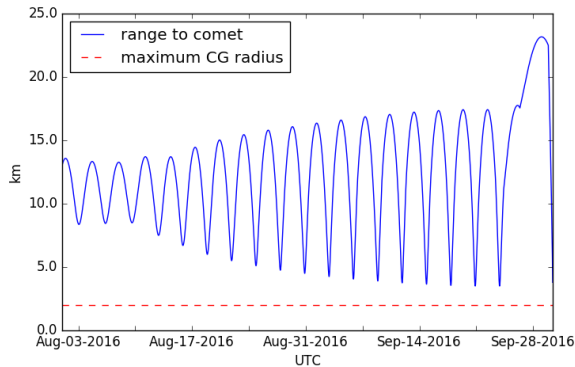


Fig. 2. Distance between Rosetta and the CG center-of-mass during the JPL support. CG has a maximum radius of about 2.0 km.

is shown in Fig. 2. This sequence of orbits allowed the navigation team the opportunity to steadily improve the estimate of the harmonic gravity coefficients up through 5th order.

On Sep. 26, Rosetta executed a maneuver to depart from the 3-day orbit in order to prepare for landing. The orbit period was increased, and the plane was oriented such that the spacecraft would move farther to the Sun-side of the comet. Rosetta was set on a collision course with the comet from about 20 km altitude in a manner very similar to that of Philae in 2014.<sup>2,3)</sup> The chosen landing site was on the north side of the smaller lobe of CG. The Rosetta spacecraft successfully landed on the comet surface at a vertical velocity around 86 cm/sec at 10:39:34 UTC on Sep. 30, 2016.<sup>3)</sup>

### 3. JPL Navigation Approach

The JPL navigation team was invited to provide only OD support for the Rosetta mission\*. As such, the JPL team had two primary subteams: Optical Navigation and Orbit Determination. The Optical Navigation (OpNav) team was responsible for creating and maintaining a model of the CG surface and for identifying landmarks from that surface in imagery downlinked from the spacecraft. The Orbit Determination (OD) team was responsible for solving for the spacecraft location relative to CG, estimating parameters of the spacecraft's dynamical environment (e.g., CG gravity field, etc.), and predicting the future path of the spacecraft using all available measurements.

The discussion here primarily focuses on the challenges and results associated with the OD activity. The complexities associated with the OpNav team's effort not documented here were significant. Some understanding of similar OpNav processes can be found in the papers covering the previous Rosetta support<sup>9)</sup> and the Dawn mission efforts.<sup>10)</sup>

#### 3.1. Dynamical Model

For the purposes of OD, the dynamical model used to integrate the spacecraft motion and partial derivatives included the following forces:

- **CG spherical-harmonic gravity model** A 12th-order model was used for propagation. The initial values of the

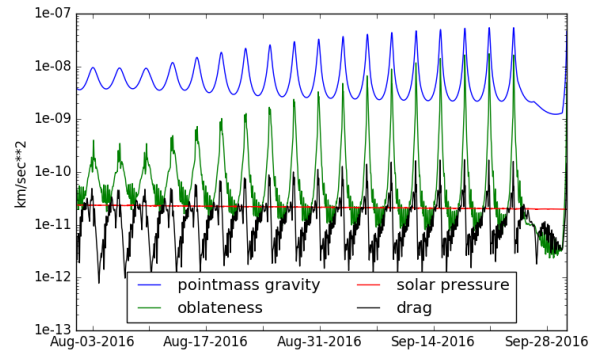


Fig. 3. Magnitudes of the various modeled accelerations acting on the spacecraft over time.

coefficients were derived assuming constant density<sup>11)</sup> and using a shape model published by ESOC-FD.<sup>12)</sup>

- **Pointmass gravity** Included for the Sun, eight planets, the Moon, and Pluto.
- **Solar-radiation pressure** A 6-panel bus model with 2 articulated solar panels were used, each with their own area and specular/diffuse coefficients. Bus and panel orientations were provided by ESOC-FD.
- **CG coma-drag model** Coma drag estimates were based on ROSINA instrument data<sup>13)</sup> when that data was available; otherwise, a coma density and velocity model derived from previous flight data was used<sup>14)</sup> in concert with the modeled spacecraft shape and orientation.
- **Impulsive  $\Delta V$  maneuvers** Planned spacecraft maneuvers were small enough that the impulsive assumption was reasonable.
- **Impulsive reaction-wheel off-load (WOL) maneuvers** These maneuvers nominally had zero magnitude due to Rosetta's balanced thruster configuration.
- **Stochastic accelerations** Short interval ( $\sim 1$  hr) acceleration batches were applied to help fit poorly modeled dynamics (such as those during low periapses or during periods of strong comet outgassing) toward the end of our support.

The relative magnitudes of these forces are shown in Fig. 3. It can be seen that the pointmass gravity of CG is overwhelmingly the dominant force on the spacecraft. As the periapsis altitudes became lower and lower, the higher-order harmonic gravity accelerations ("oblateness"), became increasingly important. In fact, the oblateness was the most important factor because its uncertainty was much larger than the uncertainty in the comet mass. Due to its close proximity to the terminator, Rosetta's drag force was a relatively small effect; the coma density is lower at the terminator and the solar panels are oriented edge-on to the outgassing velocity. Finally, solar pressure (SRP) is a relatively small effect. Generally, we did not estimate a scale factor on SRP since the expected error was on the order of  $1 \times 10^{-12}$  km/sec<sup>2</sup>.

#### 3.2. OD Filter Setup

During the 2016 JPL support, there were 2-way Doppler, 2-way Range, and on-board imagery from Rosetta's NAVCAM<sup>15)</sup> available for OD. As with all current JPL missions, the MONTE software suite<sup>16)</sup> was used for all aspects of OD and analysis.

\* The trajectory and maneuver design components of a complete navigation effort were not included.

The 2014 support of the Philae landing<sup>8)</sup> and the follow-on post-processing work provided a good starting point for the filter setup. That said, the filter strategy continued to evolve as the periapsis altitudes became lower and as the existing setup proved wanting in one way or another. Table 1 describes the parameters that were estimated or considered at one time or another. Note that not all parameters were solved for regularly and the *a priori* sigma values used were not always the same.

Table 1. OD Filter Parameters.

Parameter	Typical <i>a priori</i> 1- $\sigma$
CG-relative position (EME2000)	10 km per axis
CG-relative velocity (EME2000)	1 m/s per axis
CG gravitational parameter	0.2%
CG gravity harmonics	0.2
SRP scale factor	5%
Prime Meridian	5 deg
Rotation rate	1 deg/day
Rotation acceleration	1 deg/day <sup>2</sup>
RA / DEC of the CG spin pole	0.2 deg
Per-picture pointing error	0.005 deg
Radial landmark scale factor	0.33%
CoM-CoF offset	20 m along spin axis, 5 m otherwise
Ephemeris SetIII parameters	10x the formal covariance <sup>17)</sup>
Impulse burn $\Delta V$	5% magnitude per component
Impulse burn time	2 sec
Wheel offload $\Delta V$	0.3 mm/s

Throughout our support, we would consider several different filter setups and several data arc lengths for each OD delivery. In August, we were typically delivering solutions with a data arc of about 2 weeks, which was a good balance between the dynamical parameter accuracy achieved with a longer arc and the better terminal state accuracy achieved with a short arc. In September, however, it eventually became impossible to converge an arc longer than 2 orbits (or 6 days) due to extreme trajectory sensitivity (more on this later). Also, as the effect of gravity harmonics became more pronounced, we limited the number of parameters estimated to avoid overfitting the measurements. Aside from these challenges, our filter setup was always successful in generating a fit with flat and zero-mean residuals.

### 3.3. Optical Navigation Approach

The JPL OpNav team was able to use the navigation shape model they generated in 2014<sup>9)</sup> as the initial basis for the 2016 effort. In the spring and summer of 2016, the 2014 shape model was updated based on Rosetta NAVCAM images<sup>15)</sup> obtained in early 2016. The update proved to be more challenging than expected because the rotation rate for CG was not constant due to comet outgassing activity<sup>18)</sup> and because the fine detail of the comet surface had been changed by the outgassing activity during perihelion.

During the operational period, the OpNav team had two important roles in the OD process. The first was to maintain and improve the comet navigation shape model. As in previous missions,<sup>9,10)</sup> this was done using the stereo-photoclinometry

(SPC) technique.<sup>19)</sup> In short, this technique estimates a best-fit topography and albedo model for a collection of surface patches (“landmarks”) based on all available imagery of those locations (with boundary conditions enforced to ensure a continuous global shape model). The resulting model can be combined with an assumed reflection law to predict what future images of that patch of surface look like under any lighting conditions. The second role of the OpNav team is to identify landmarks in NAVCAM images as they come down to be used as measurements. Using a rotation model of the comet and camera pointing information, landmark observations are used to effectively triangulate the spacecraft position at the time of the image. These landmark observations are powerful measurements for determining the spacecraft state relative to the comet.

## 4. Trajectory Estimation

The goals of orbit determination are to reconstruct where the spacecraft has been and to predict where the spacecraft will go in the future. On both points, the formal covariance result from the filter is typically presented as a measure of the solution accuracy. However, the accuracy of the formal covariance relies on the setup of the filter and its inputs. In order to get an accurate formal covariance, the dynamical model must accurately represent reality using the estimated parameters and the covariances associated with them. Input covariances must be properly correlated when appropriate (e.g., different landmark observations in the same image). Our experience has demonstrated that the model we use in our filter is not yet accurate enough to generate accurate formal covariances. Generally, the formal covariances have been found to be overly optimistic. Since the true trajectory of the spacecraft is not known, we assess the quality of our navigation solutions here by comparing against subsequent solutions and not against the predicted covariance.

Figure 4 shows the position differences between all OD solution pairs during times when the respective data arcs overlap. Since both solutions utilize the same measurements during the overlap, the plotted position differences give an empirical estimate of the precision of our reconstructed trajectories. The true accuracy of our solutions may be worse than this due to biases introduced by our filter setup, but it is no better. It can be seen that generally our results were precise at the 20 meter level or better. August yielded more precise results than were achieved in September, but this is likely because the OD was not as challenging. The precision began to degrade as the periapsis altitude decreased primarily due to the increasing influence of the poorly-estimated high-order gravity terms.

In Fig. 5, the position difference is shown between each OD solution’s 3-day prediction and the subsequent trajectory solution. Since the subsequent trajectory should be relatively close to the truth (as it contains measurements throughout the 3-day period), this plot is a good representation of the accuracy of our trajectory predictions over 3 days. It can be seen from the plot that predictions were typically accurate to 50 meters or better in the first 24 hours leading up to periapsis. A clear local maximum can be seen around 40 hours, which corresponds to the first periapsis in the 3-day orbits (Fig. 1). After periapsis, we typically had a residual orbit-period error that resulted in a consistent and rapid increase in position error. We did not figure

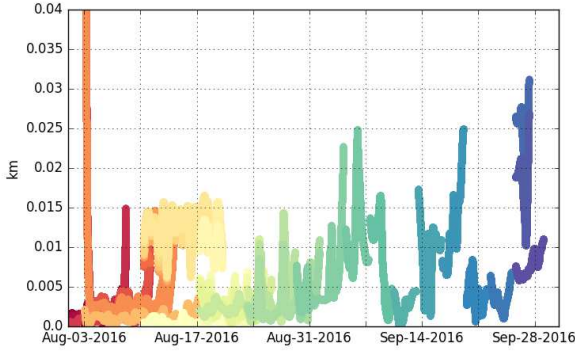


Fig. 4. Precision of JPL operational OD solutions. Trajectory estimates are compared at times when the data arc from multiple solutions overlap. Each colored line shows the difference between two overlapping OD data arcs.

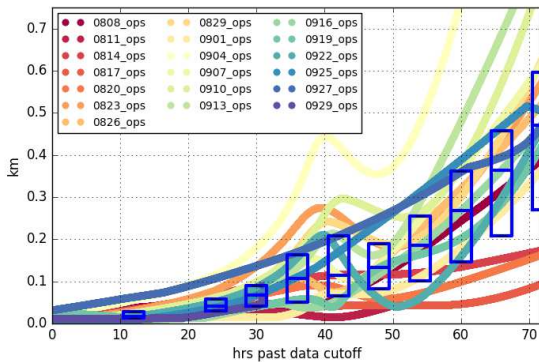


Fig. 5. Prediction accuracy of JPL operational OD solutions as a function of hours past data cutoff. 3-day trajectory predictions for each solution are compared against the next operational solution (which has measurements during the prediction). The blue boxes show the 25th, 50th, and 75th percentiles of the resulting errors in 6-hour increments. The labels indicate the month and day of the data cutoff (MMDD format).

out how to address this issue. After one 3-day orbit, our position prediction errors were typically 300-600 meters.

## 5. Parameter Estimation

Our estimates for the majority of the parameters in Table 1 are not generally useful to report (e.g., spacecraft epoch states, internal shape model adjustments, per-picture pointing corrections, maneuver solutions, etc.). We will present our gravity harmonic estimates to help give future missions a sense of the accuracy they may be able to achieve during operations for a similar mission and to compare with the high-fidelity reconstruction to come. Also, the migration of our operational spin pole estimate may be of use as a point of comparison with other results presented.<sup>3,6)</sup>

### 5.1. Gravity Estimation

Figure 3 demonstrates the increasing importance of a good high-order harmonic gravity model over the course of the 2016 support. The GM and the 2nd order harmonics were readily observable throughout the month of August and we quickly derived reliable estimates. Estimating the higher-order harmonics was complicated by our inability to fit multiple orbits in one

data arc when the periapsis was low (i.e., when the information content was the highest). We ultimately adopted an approach of estimating the gravity harmonics separately from the operational OD filter. In this separate filter, we combined the information from each periapsis passage (between OCMs) independently. By mid-September, we had derived a reliable estimate of the 3rd order harmonics that improved our predictions noticeably. By the time of landing, we also derived a set of 4th and 5th order coefficients that showed a clear improvement in the accuracy of our predictions (though the formal covariances indicated significant uncertainty in those estimates). Table 2 presents our gravity results through 3rd order. The reference radius here is 1.0 km, the origin is at the center of mass, the z-axis is aligned with the maximum moment of inertia, and the CHEOPS reference frame is used.<sup>20) †</sup>

Table 2. Estimated CG Gravity Harmonics (CHEOPS frame).

GM	$(6.651 \pm .003) \times 10^{-7} \text{ km}^3/\text{sec}^2$		
J2	$0.2350 \pm 0.0036$	J3	$0.1250 \pm 0.0123$
C22	$0.3210 \pm 0.0054$	S22	$-0.0165 \pm 0.0043$
C31	$-0.1487 \pm 0.0089$	S31	$0.0655 \pm 0.0097$
C32	$0.2066 \pm 0.0165$	S32	$-0.0874 \pm 0.0156$
C33	$0.0281 \pm 0.0245$	S33	$-0.3580 \pm 0.0244$

### 5.2. Spin Pole Estimation

Figure 6 shows the variation in our operational spin pole estimates. It can be seen that the estimated values for both right ascension and declination sometimes exceed the formal 3-sigma uncertainties of previous solutions. This may be because the covariances are overly optimistic or because the pole has moved due to comet outgassing torques. It may also be due to an unrelated mismodeling in the filter. Note that the large formal uncertainties for the 0904 through 0910 solutions correspond to solutions that solved for a spin acceleration, which increased the uncertainty in the spin rate estimate. The 5- to 15-day data arcs for these solutions is probably too long to clearly show the effect of the 11-day precession effect that has been described elsewhere.<sup>18,20)</sup>

### 5.3. Rosetta Landing Results

Our estimated terminal trajectory matched to about 12 meters with the estimate from ESOC-FD in the final moments of the descent. The difference was effectively all in the radial / time-of-flight direction. Using our trajectory and independent shape model, we estimated a landing time of 30-SEP-2017 10:38:12 UTC, which was about 82 seconds earlier than the observed loss-of-signal from the spacecraft that indicated touchdown.<sup>3)</sup>

## 6. Orbit Determination Challenges

Rosetta was the first mission to ever navigate a spacecraft in orbit around a comet. There are many unique aspects of this environment that give rise to many unique navigation issues. There also were challenges induced (and avoided) through the particular design of the Rosetta mission and challenges that the JPL team imposed upon itself. This following topics are discussed in no particular order.

<sup>†</sup> The estimated CG mass decreased noticeably relative to the 2014 result.<sup>8)</sup> This may well be due to the comet outgassing. Ref. 21) estimates the water loss during perihelion passage was  $6.4 \times 10^9 \text{ kg}$ , or about  $4.3 \times 10^{-10} \text{ km}^3/\text{sec}^2$ .

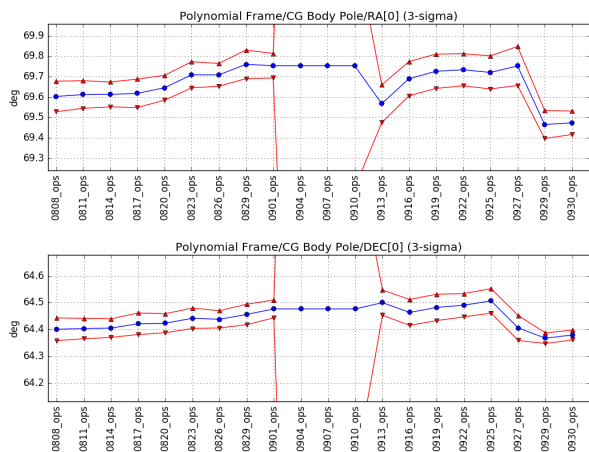


Fig. 6. Operations estimates of CG spin pole right ascension and declination (J2000). The blue line gives the estimated value and the red lines give the formal 3-sigma boundaries.

### 6.1. Orbit Determination Challenges at a Comet

The most obvious navigation challenge associated with a comet is modeling the drag acceleration on the spacecraft resulting from the comet outgassing activity. The coma density and velocity model provided to us by ESOC for the 2016 support<sup>14)</sup> proved that the comet activity can be modeled reasonably well based on *in situ* observations, given enough of them. The ROSINA instrument<sup>13)</sup> provided the measurements for that model, so it was a boon to navigation to have that instrument onboard the spacecraft. When the data was available, we used the ROSINA data directly to model the coma density in our reconstructions.

Given a good model of the coma density and velocity, a model is still required for how the flow field interacts with the spacecraft shape to result in a drag acceleration. In 2014, the JPL team experimented with both a single parameter “cannonball” drag model (where drag acceleration is always in the opposite direction of the flow relative velocity) and a two parameter lift and drag model. The lift-drag model was never shown to be any better than the cannonball model in the 2014 effort.<sup>8)</sup> Combined with the secondary significance of the drag relative to the high-order gravity effects (Fig. 3), the JPL used the cannonball model throughout the 2016 support.

It is also worth noting that the comet outgassing is not always consistent over time and occasional outbursts of particularly strong effects should be accounted for in the navigation strategy. On Sep. 5, one such outburst occurred. These events can be detected through inspection of the pre- and post-fit Doppler residuals. We made use of short-batch stochastic accelerations to estimate the resulting spacecraft accelerations.

Another interesting effect of comet outgassing is that it places a torque on the comet. This results in a change in spin rate over time and a change in the spin pole over time. Late in the 2014 support, we realized that the rotation rate was indeed changing. We didn’t have enough insight into the outgassing activity to parameterize a torque model for the comet, which might have been the ideal approach. Our approach to deal with a changing spin rate in 2016 was to either limit the length of our solution arcs or to estimate a constant acceleration on the spin. Neither

solution provides a suitable model for use in a long arc solution. We also updated the epoch for the initial prime meridian of the spin every few weeks to keep the uncertainty in that initial prime meridian angle from getting too big.

The spin-pole of CG may or may not have been stable, possibly due to outgassing torques. Several papers<sup>18,20)</sup> have identified a precession term in the pole motion, but this was not clearly observable in our navigation solutions. We did observe that our solutions for the comet pole were not consistent over time, as presented previously (Fig. 6). This lack of consistency was also observed by our team in 2014 and the ESOC-FD team.<sup>4)</sup> The pole motion we observed may or may not have been due to outgassing torque or the induced precession.

### 6.2. Rosetta specific challenges

The mass distribution of CG was irregular, even by primitive body standards. When operating at 10 km range or more (as in 2014), the gravitational potential can be well modeled using a constant density assumption and estimating spherical harmonic parameters up to 3rd order or so. In the 2016 support, Rosetta flew as low as ~2 km altitude and the high-order irregular gravity effects became very significant. The Rosetta trajectory design anticipated the challenge of estimating the high-order terms and lowered the periapsis gradually to accommodate. This was helpful, but it was still difficult to fit the Doppler and range measurements around periapsis until there was enough data at that altitude to get a good estimate of the corresponding harmonics.

We also had difficulty fitting measurements over more than 2 Rosetta orbits starting in early September. After two orbits, the computed measurement values became very sensitive to velocity changes at the start of the data arc. If we tried to fit more than 2 orbits, the filter would initially appear to converge normally, but ultimately fail to converge. We hypothesize that this was due to an extreme sensitivity in the computed measurement (optical or Doppler) to velocity changes early in the data arc. The sensitivity was so extreme that the precision limitations of the computer resulted in bad partial derivatives and bad parameter updates which caused the filter to diverge. In the early orbits, we did not have this problem, but as the orbit became more eccentric, the sensitivity of the spacecraft state to epoch state velocity changes increased.

For each 3-day orbit during the 2016 support, the spacecraft performed two planned deterministic maneuvers and three reaction wheel desaturation maneuvers. Generally, the more maneuvers a spacecraft does, the harder it is to solve for dynamic parameters, such as gravity harmonics, because the uncertainty introduced by the maneuver execution can be larger than the subtle effect of an error in the dynamics. For Rosetta, that was indeed occurring, but it may have actually been a good thing. Since it is almost impossible to model the coma drag effect perfectly, the maneuvers gave the filter a parameter that could absorb any unmodeled coma drag effects. While this degraded the accuracy at which we might have estimated gravity, it gave the filter an opportunity to prevent spacecraft velocity errors from accumulating over time.

The 3-day orbit period was nearly resonant with the 12.054 hr rotation period of CG. Thus, the body-fixed longitude of the periapses during this phase of improving gravity field knowledge only moved about 10 deg per orbit. It was unclear how this affected the quality of the higher-order gravity field estimates,

but it is probable that the estimated harmonics would have performed more poorly at significantly different longitudes. Fortunately, this really didn't matter for navigation because we didn't fly the spacecraft at those longitudes. An advantage of the repeating orbit geometry is that we were able to apply an empirical approach to comparing different filter designs.

### 6.3. JPL-specific challenges

In 2014, we had an issue where the overall scale of our comet model was incorrect. This manifested itself in an inability to fit both the radiometric and the optical data well at the same time. We corrected the problem in October of 2014 to good effect. Throughout 2016, we regularly estimated a scale factor across all the optical landmarks and that seems to have worked well. Similarly, we consistently estimated a center-of-mass to center-of-figure offset to account for the inability of the SPC process to determine the CG center of mass.

Our post-operations analysis demonstrably show that our trajectory reconstructions, trajectory predictions, and the consistency in our parameter estimates clearly improved since the 2014 effort as we incorporated the lessons we learned then. That said, we still found comet navigation to be quite challenging. Particularly notable is that our predictions generally were not as good as our formal covariance mappings suggested and they weren't as good as those generated by ESOC-FD during the orbits with lower periapses. Figuring out the reasons for this is a topic for future work for our team.

## 7. Conclusions

JPL's second "shadow navigation" experience with the Rosetta spacecraft at comet 67P/Churyumov-Gerasimenko has been reviewed. The effort was certainly a success in the sense that we continued to expand on our understanding of the navigation challenges associated with close-proximity operations at a comet. This paper has attempted to present both our struggles and our successes for the benefit of future efforts.

## 8. Acknowledgments

The authors would like to thank our colleagues in the Flight Dynamics group at the European Space Operations Center for the invitation to participate in this historic mission, for the outstanding opportunity to work with real navigation data from a cometary environment, and for the free exchange of ideas.

The work described in this paper was carried out at the Jet Propulsion Laboratory, California Institute of Technology, under a contract with the National Aeronautics and Space Administration.

## References

- Glassmeier, K.-H., Boehnhardt, H., Koschny, D., Kührt, E., and Richter, I.: The Rosetta Mission: Flying Towards the Origin of the Solar System, *Space Science Reviews*, **128** (2007), pp. 1-21.
- Accomazzo, A., Lodi, S., and Companys, V.: Rosetta mission operations for landing, *Acta Astronautica*, **125** (2016), pp. 30-40.
- Accomazzo, A., Ferri, P., Lodi, S., Pellon-Bailon, J.-L., Hubault, A., Urbanek, J., Kay, R., Eiblmaier, M., and Francisco, T.: The final year of the Rosetta mission, *Acta Astronautica*, **136** (2017), pp. 354-359.
- Godard, B., Budnik, F., Muñoz, P., Morley, T., and Janarthanan, V.: Orbit Determination of Rosetta Around Comet 67P Churyumov-Gerasimenko, 2015 International Symposium on Space Flight Dynamics, Munich, Germany, 2015.
- Muñoz, P., Budnik, F., Companys, V., Godard, B., Casas, C.M., Morley, T., and Janarthanan, V.: Rosetta Navigation During Lander Delivery Phase and Reconstruction of Philae Descent Trajectory and Rebound, 2015 International Symposium on Space Flight Dynamics, Munich, Germany, 2015.
- Godard, B., Budnik, F., Bellei, G., Muñoz, P. and Morley, T.: Multi-arc Orbit Determination to determine Rosetta trajectory and 67P physical parameters, 2017 International Symposium on Space Flight Dynamics, Matsuyama, Japan, ISSFD-2017-095, 2017.
- Muñoz, P., Companys, V., Budnik, F., Godard, B., Pelleginetti, D., Bellei, G., Bauske R., and Martens, W.: Rosetta Navigation during the End of Mission Phase, 2017 International Symposium on Space Flight Dynamics, Matsuyama, Japan, ISSFD-2017-015, 2017.
- Bhaskaran, S., Broschart, S., Han, D., Owen, B., Mastrodemos, N., Roundhill, I., Rush, B., Surovik, D., Budnik, F., and Companys, V.: Rosetta Navigation at Comet Churyumov-Gerasimenko, AAS Guidance, Navigation, and Control Conference, Breckenridge, Colorado, AAS 15-122, 2015.
- Mastrodemos, N., Rush, B.P., Owen, W.M. Jr.: Optical Navigation for the Rosetta Mission, AAS Guidance, Navigation, and Control Conference, Breckenridge, Colorado, AAS 15-123, 2015.
- Mastrodemos, N., Rush, B.P., Vaughan, A.T., Owen, W.M. Jr.: Optical Navigation for Dawn at Vesta, AAS/AIAA Space Flight Mechanics Meeting, New Orleans, Louisiana, AAS 11-222, 2011.
- Werner, R.A.: Spherical Harmonic Coefficients for the Potential of a Constant-density Polyhedron, *Computers and Geosciences*, **23** (1997), pp. 1071-1077.
- ESA NAVCAM Shape Model, OBJ File (3,6 MB), [http://imagearchives.esac.esa.int/index.php?page/navcam\\_3d\\_models](http://imagearchives.esac.esa.int/index.php?page/navcam_3d_models) (accessed Apr. 2017).
- Balsiger, H., Altwegg, K., Arijis, E., Bertaux, J.-L., Berthelier, J.-J., Bochsler, P., Carignan, G.R., Eberhardt, P., Fisk, L.A., Fuselier, S.A., and others: Rosetta Orbiter Spectrometer for Ion and Neutral Analysis - ROSINA, *Advances in Space Research*, **21** (1998), pp. 1527-1535.
- Bielsa, C., Müller, M., and Herfort, U.: Operational Approach for the Modeling of the Coma Drag Force on Rosetta, 2014 International Symposium on Space Flight Dynamics, Laurel, Maryland, 2014.
- Geiger, B., Barthelemy, M., and Archibald, C.: ROSETTA-NAVCAM to Planetary Science Archive Interface Control Document, European Space Agency Internal Document RO-SGS-IF-0001, v5.3, 2016. <https://pdssbn.astro.umd.edu/holdings/ro-c-navcam-2-ext3-mtp035-v1.0/document/ro-sgs-if-0001.pdf>.
- Evans, S., Taber, W., Drain, T., Smith, J., Wu, H.-C., Guevara, M., Sunseri, R., and Evans, J.: MONTE: The Next Generation of Mission Design & Navigation Software, 6th International Conference on Astrodynamics Tools and Techniques, Darmstadt, Germany, 2016.
- JPL Small-Body Database Browser, 67P/Churyumov-Gerasimenko ephemeris solution K084/25 created on July 13, 2016 by Ryan Park, <http://ssd.jpl.nasa.gov/sbdb.cgi> (accessed Jul. 2016).
- Jorda, L., Gaskell, R., Capanna, C., Hviid, S., Lamy, P., Āurech, J., Faury, G., Groussin, O., Gutiérrez, P., Jackman, C., and others: The global shape, density and rotation of Comet 67P/Churyumov-Gerasimenko from preperihelion Rosetta/OSIRIS observations, *Icarus*, **277** (2016), pp. 257-278.
- Gaskell, R.W., Barnouin-Jha, O.S., Scheeres, D.J., Konopliv, A., Mukai, T., Abe, S., Saito, J., Ishiguro, M., Kubota, T., Hashimoto, T., and others: Characterizing and navigating small bodies with imaging data, *Meteoritics and Planetary Science*, **43** (2008), pp. 1049-1061.
- Preusker, F., Scholten, F., Matz, K.-D., Roatsch, T., Willner, K., Hviid, S.F., Knollenberg, J., Jorda, L., Gutiérrez, P.J., Kührt, E., and others: Shape model, reference system definition, and cartographic mapping standards for comet 67P/Churyumov-Gerasimenko—Stereophotogrammetric analysis of Rosetta/OSIRIS image data, *Astronomy & Astrophysics*, **583** (2015), pp. A33.
- Hansen, K.C., Altwegg, K., Berthelier, J.-J., Bieler, A., Biver, N., Bockelée-Morvan, D., Calmonte, U., Capaccioni, F., Combi, M.R., De Keyser, J., and others: Evolution of water production of 67P/Churyumov-Gerasimenko: An empirical model and a multi-instrument study, *Monthly Notices of the Royal Astronomical Society*, (2016), pp. stw2413.